Composites: Part B 43 (2012) 3160–3166

Contents lists available at SciVerse ScienceDirect

Composites: Part B

journal homepage: www.elsevier.com/locate/compositesb

The influence of heterogeneous meninges on the brain mechanics under primary blast loading

Linxia Gu [a,b,*], Mehdi S. Chafi [a], Shailesh Ganpule [a], Namas Chandra [a]

[a] Department of Mechanical and Materials Engineering, University of Nebraska–Lincoln, Lincoln, NE 68588-0656, United States
[b] Nebraska Center for Materials and Nanoscience, Lincoln, NE 68588-0656, United States

ARTICLE INFO

Article history:
Received 2 September 2011
Received in revised form 11 January 2012
Accepted 13 April 2012
Available online 20 April 2012

Keywords:
A. Layered structures
B. Mechanical properties
B. Interface/interphase
C. Finite element analysis
Blast wave

ABSTRACT

In the modeling of brain mechanics subjected to primary blast waves, there is currently no consensus on how many biological components to be used in the brain–meninges–skull complex, and what type of constitutive models to be adopted. The objective of this study is to determine the role of layered meninges in damping the dynamic response of the brain under primary blast loadings. A composite structures composed of eight solid relevant layers (including the pia, cerebrospinal fluid (CSF), dura maters) with different mechanical properties are constructed to mimic the heterogeneous human head. A hyper-viscoelastic material model is developed to better represent the mechanical response of the brain tissue over a large strain/high frequency range applicable for blast scenarios. The effect of meninges on the brain response is examined. Results show that heterogeneous composite structures of the head have a major influence on the intracranial pressure, maximum shear stress, and maximum principal strain in the brain, which is associated with traumatic brain injuries. The meninges serving as protective layers are revealed by mitigating the dynamic response of the brain. In addition, appreciable changes of the pressure and maximum shear stress are observed on the material interfaces between layers of tissues. This may be attributed to the alternation of shock wave speed caused by the impedance mismatch.

1. Introduction

Blast-related traumatic brain injury (TBI), including injuries caused form primary shock waves, penetration, impact, and fire/toxic gases, is a common injury in the course of current military conflicts. A study on a combat brigade returning from Iraq showed that 22.8% of soldiers had at least one TBI confirmed by a clinician, and more importantly, 88% of those injuries were caused by exposure to blasts resulting from improvised explosive devices [1]. Understanding the mechanisms of TBI is necessary for developing more appropriate protective systems and diagnostic tools.

Finite element (FE) analysis has emerged as a powerful tool for investigating injuries of the human head under different loading conditions. The level of geometric complexity, constitutive equations and material properties determines the accuracy of blast–head interaction results. The brain floats within the skull surrounded by CSF and meninges layers that allows for relative motion between the brain and the skull. This movement caused the rupture of bridging veins, which account for the majority of TBI [2]. A previous study examined the role of CSF properties on the response of human brain under certain impact loadings [3]. To the best of our knowledge, no published data is available on the role of meninges in transferring blast impacts to the brain. There is no consensus on including meninges [4,5] or not [6,7]. There is also no discussion on the right biological components required to be included in the blast FE models. Different biological components within the head (i.e., skull, dura and arachnoid mater, CSF, pia mater, and brain) have different densities with many interfaces separating these components with varying magnitudes of acoustic impedances. Recent findings have shown that shock waves are reflected/transmitted/converted at heterogeneous interfaces and their ratios directly depend on the mismatch in acoustic impedance at the surface of separation [8]. Further, the frequency content of the sharply rising shock wave overpressure dictates the spatial resolution at which the impedance mismatch becomes pronounced. For example, a wave with a frequency in the MHz range will have three orders of higher spatial resolution compared to a frequency in the kHz range wherein the waves either reflect, transmit or split [9].

The aim of this study is to investigate the influence of the structural heterogeneities of the human head on damping the dynamic response of the brain under primary blast loading conditions. Two-dimensional plane strain FE models with detailed geometries of the human head, including meninges and CSF, have been developed using an explicit nonlinear dynamic code LS-DYNA (Livermore

* Corresponding author at: Department of Mechanical and Materials Engineering, University of Nebraska–Lincoln, Lincoln, NE 68588-0656, United States. Tel.: +1 402 472 7680; fax: +1 402 472 1465.
E-mail address: lgu2@unl.edu (L. Gu).

1359-8368/$ - see front matter
http://dx.doi.org/10.1016/j.compositesb.2012.04.014

Software Technology Corporation, Livermore, CA, USA). This model is used to carry out parametric studies in order to help understand the influence of material models of pia maters, dura maters, and CSF on the dynamic response of brain.

2. Material and methods

Anatomically, human brain is encased in the triple layers of skull (outer table, diploe and inner table) and is suspended and supported by a series of three fibrous tissue layers, dura mater, CSF and pia mater, known as the meninges, as shown in Fig. 1. The FE model is composed of 6700 8-nodded solid elements including Eulerian elements to represent the CSF. A summary of the material properties for the various tissue layers is listed in Table 1.

Though the selection of the material model is critical in the analysis of the response of shock wave, there is no published work that examines the selection of the right material model for the intracranial components. This requirement is exacerbated by the fact that the material model should be valid for the brain tissue over a large strain/high frequency range encountered in blast loading scenarios. In this paper, a hyper-viscoelastic material model for the brain is employed over a large strain/high frequency range. The model is formulated in terms of a large strain viscoelastic framework and considers linear viscous deformations in combination with non-linear hyperelastic behavior. This Cauchy stresses from both hyperelastic and viscoelastic frameworks are superimposed onto each other to describe the brain behavior.

For the hyperelastic part of the material model, an Ogden hyperelastic strain energy function for incompressible material is adopted to describe the strain-dependent mechanical properties of brain tissue. The resulted Cauchy stress tensor σ is then calculated as:

$$\sigma = \frac{\partial W}{\partial \varepsilon} = \frac{\partial\left[\sum_{i=1}^{N}\frac{\mu_i}{\alpha_i}\left(\lambda_1^{\alpha_i}+\lambda_2^{\alpha_i}+\lambda_3^{\alpha_i}-3\right)\right]}{\partial \varepsilon} \tag{1}$$

where W is the Ogden strain energy function, ε is the Green strain tensor. λ_1, λ_2, and λ_3 are the principal stretch ratios, and μ_i and α_i are constants to be determined experimentally for each value of i.

Four Ogden hyperelastic parameters were determined from the reported experimental data [10] as $\mu_1 = -132.6$ kPa, $\mu_2 = 0.481$ kPa, $\alpha_1 = 0.00374$, and $\alpha_2 = 10.01$. A comparison between the experimentally obtained stress–strain curve [11] and mathematically fitted one is shown in Fig. 2. The agreement between numerical and experimental data appears to be quite good.

For the viscoelasticity part of the material model, the linear Maxwell is adopted and its associated Cauchy stress is computed through the following equation:

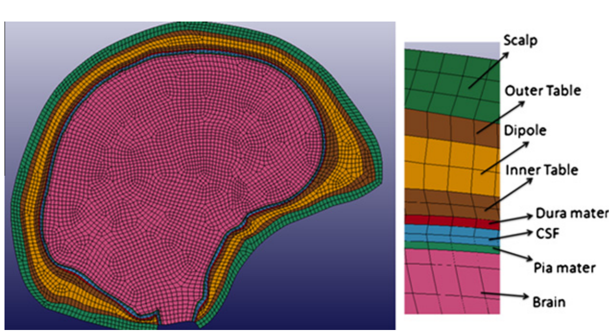

Fig. 1. FE model arrangement with heterogeneous geometry and initial mesh of the model including triple layers of the skull (two cortical layers and middle diploe sponge-like layer), dura mater, cerebrospinal fluid (CSF), pia mater and the brain.

$$\sigma_{ij} = JF_{ik}^{T}\cdot S_{km}\cdot F_{mj} \tag{2}$$

where σ_{ij} is the Cauchy stress component, F is the deformation gradient tensor, and J is the transformation Jacobian. The second Piola–Kirchhoff stress S_{ij} was estimated by a convolution integral of the form as:

$$S_{ij} = \int_0^t G_{ijkl}(t-\tau)\frac{\partial E_{kl}}{\partial \tau}d\tau \tag{3}$$

where E_{kl} is the Green's strain tensor, and $G_{ijkl}(t-\tau)$ is the relaxation modulus function for the different stress measurements, which can be represented in terms of the Prony series:

$$G(t) = G_0 + \sum_{i=1}^{n} G_i e^{-\beta_i t} \tag{4}$$

where G_i is the relaxation modulus and β_i is the decay constant.

The relaxation moduli and decay constants are also derived from the published experimental data [11–17] at a wide frequency range between 0.01 MHz and 10 MHz. The fitted six term Prony series material parameters are: G_∞ = 2160 Pa, G_1 = 156,488.3 kPa, G_2 = 326,025.8 kPa, G_3 = 0.0016 kPa, G_4 = 1.2313 kPa, G_5 = 17.583 kPa, G_6 = 0.0254 kPa, β_1 = 1.0763e + 9 s^{-1}, β_2 = 35.7999e + 6 s^{-1}, β_3 = 383.5146e + 3 s^{-1}, β_4 = 1e + 3 s^{-1}, β_5 = 10 s^{-1}, and β_6 = 3.6533 s^{-1}.

The numerical and experimental data are presented in Fig. 3. More terms of Prony series can be used to obtain a better fit, however the six terms in the Prony series expansion is the limit in the commercial FE code LS-DYNA. In summary, the hyper-viscoelastic material model of the brain is depicted by seventeen material parameters in this work. This is the first material model for the brain that covers such wide range of frequencies.

The skull is modeled as a three-layered non-homogeneous material, including two cortical layers, i.e., outer table and inner table, and middle diploe sponge-like layer. Each layer is modeled as an isotropic material with properties listed in Table 1. A Gruneisen equation of state was used to mimic the behavior of CSF with a bulk modulus of 2.19 GPa. An equation of state (EOS) determines the hydrostatic behavior of the material by calculating pressure as a function of density, energy, and/or temperature and represented by Eq. (5) in most generic form.

$$p = \frac{\rho_0 C^2 \mu\left[1+\left(1-\frac{\gamma_0}{2}\right)\mu - \frac{a}{2}\mu^2\right]}{\left[1-(S_1-1)\mu - S_2\frac{\mu^2}{\mu+1} - S_3\frac{\mu^3}{(\mu+1)^2}\right]} + (\gamma_0 + a\mu)E \tag{5}$$

where $\mu = \frac{\rho}{\rho_0} - 1 = \frac{1}{V_0} - 1$. C and S_1 are parameters in the shock velocity (v_s) and particle velocity (v_p) according to the relation: $v_s = C + S_1 v_p$. C is the intercept of the v_s–v_p curve, S_1, S_2, and S_3 are the coefficients of the slope of the v_s–v_p curve. Additionally, γ_0 is the Gruneisen gamma, a is the first order volume correction to γ_0 and E is the internal energy. In this work, S_1, S_2, S_3, γ_0 and a are set to zero.

The mechanical properties of the meninges layers are not well established in the literature and there is a wide range the elastic moduli attributed to them [18,19]. For dura and pia maters, a second order Ogden hyperelastic model and two elastic models based on the published experimental work [18–20] have been employed to estimate the influence of the materials, as described in Table 2 and Fig. 4. Jin et al. [19] performed uniaxial quasi-static and dynamic tensile experiments on pia mater at strain-rates of 0.05, 0.5, 5 and 100 s^{-1}. Since high strain rate data is more suitable and applicable for blast loading scenarios, the data regarding 100 s^{-1} strain rates was used to formulate the constitutive model in this study. The fitted material behaviors were added in Fig. 3.

In this study, a blast scenario characterized by positive pulse duration and peak overpressure has been used with reference to the Bowen curves, which indicated that the unprotected lung injury threshold is 5.4 atm peak pressure [21]. The simulated shock load, illustrated in Fig. 5, is associated with free-air detonation